Infrared Spectra and Density Functional Calculations for OScCO, Sc-(η^2-OC)O, OSc-(η^2-CO), and Three $OScCO^+$ Cation Isomers in Solid Argon

Mingfei Zhou and Lester Andrews*

Contribution from the Department of Chemistry, University of Virginia, Charlottesville, Virginia 22901

Received August 12, 1998

Abstract: Laser-ablated Sc atoms react with CO_2 molecules to give primarily the insertion product, OScCO, and a minor amount of the addition product, Sc-(η^2-OC)O, which have been isolated in a solid argon matrix. Photoisomerization to form the novel side-bonded OSc-(η^2-CO) isomer and photoionization to the $OScCO^+$ cation and $OScOC^+$ and $ScOCO^+$ isomers proceed upon different wavelength photolyses. The product absorptions were identified by isotopic substitution and density functional calculations of isotopic frequencies. Similar experiments with Y give spectra for the analogous product molecules and cations.

Introduction

Carbon dioxide is the most abundant carbon source in the atmosphere. Accordingly, metal catalytic activation of carbon dioxide to form organic compounds is receiving increased attention.[1−4] The interaction of CO_2 and transition metal centers has been studied both experimentally[5−11] and theoretically.[12−16] Complexes with first-row transition metals Ti through Cu have been studied in solid CO_2,[7] and the reactions of laser-ablated Ti and Cr, Mo, W atoms with CO_2 in excess argon have been investigated in this laboratory.[17,18] These experiments indicate that early transition metals insert into CO_2 to form the OMCO molecules, while Fe and Co form the η^1-C and Cu the η^1-O coordination complexes. To our knowledge, no experimental work has investigated interactions of Sc and Y with CO_2 molecules.

Recently, two theoretical studies have been performed on the interaction of Sc atoms and CO_2 molecules,[14,15] and the structure, binding energy, and vibrational frequencies have been determined for different $ScCO_2$ structural arrangements. The inserted OScCO molecule was calculated to be the most stable isomer, followed by the η^2-OC, η^2-O,O, η^1-O, and η^1-C coordinated isomers, and it was concluded that the η^2-OC isomer will spontaneously evolve into the insertion product.[15] Finally, the calculation of Sc^+ interacting with CO_2 also shows that the inserted $OScCO^+$ structure is more stable than the addition $ScOCO^+$ isomer,[16] and this is substantiated by gas-phase investigations with V^+ cations.[8]

In this paper, we present a study of the reaction of laser-ablated Sc and Y atoms with CO_2 molecules. We will show that insertion to form OMCO is the primary reaction and that photoisomerization to the new OM-(η^2-CO) isomer and photoionization to several $OMCO^+$ cation isomers proceeds on visible and ultraviolet−visible photolysis, respectively.

Experimental Section

The experiment for laser ablation and matrix isolation spectroscopy has been described in detail previously.[19] Briefly, the Nd:YAG laser fundamental (1064 nm, 10-Hz repetition rate with 10-ns pulse width) was focused on the rotating Sc or Y metal target (Johnson Matthey, lump, 99.9%) using low-energy (3−5 mJ) pulses. Laser-ablated metal atoms were co-deposited with carbon dioxide (0.5%−1.0%) in excess argon onto a 12K CsI cryogenic window at 2−4 mmol/h for 1−2 h. Carbon dioxide (Matheson) and isotopic $^{13}C^{16}O_2$ and $^{12}C^{18}O_2$ (Cambridge Isotopic Laboratories) and $^{12}C^{16}O_2 + {}^{13}C^{16}O_2$ or $^{12}C^{16}O_2 + {}^{12}C^{16,18}O_2 + {}^{12}C^{18}O_2$ mixtures were used in different experiments. FTIR spectra were recorded at 0.5 cm^{-1} resolution on a Nicolet 750 spectrometer with 0.1 cm^{-1} accuracy using an MCTB detector. Matrix samples were annealed at different temperatures and subjected to different wavelength photolyses for 10−15-min periods using a medium-pressure mercury arc lamp (Philips, 175 W, without globe, 240−580 nm) and glass filters.

Results

FTIR spectra of the Sc + CO_2/Ar and Y + CO_2/Ar systems and DFT calculations will be presented.

Sc + CO_2/Ar. The carbon dioxide/argon samples revealed the strong allowed bands site split at 2344.8, 2339.0 and 663.5, 661.9 cm^{-1}, the weak Fermi doublet at 1383.7, 1279.5 cm^{-1},

(1) Palmer, D. A.; Van Eldik, R. *Chem. Rev.* **1983**, *83*, 651.
(2) Solymosi, F. *J. Mol. Catal*. **1991**, *65*, 337.
(3) Creutz, C., In *Electrochemical and Electrocatalytic Reactions of Carbon Dioxide*; Sullivan, B. P., Krist, K., Guard, H. E., Eds.; Elsevier: Amsterdam, 1993.
(4) Gibson, D. H. *Chem. Rev.* **1996**, *96*, 2063.
(5) Huber, H.; McIntosh, D.; Ozin, G. A. *Inorg.Chem*. **1977**, *16*, 495.
(6) Ozin, G. A.; Huber, H.; McIntosh, D. *Inorg. Chem*. **1978**, *17*, 147.
(7) Mascetti, J.; Tranquille, M. *J. Phys. Chem*. **1988**, *92*, 2173.
(8) Sievers, M. R.; Armentrout, P. B. J. *Chem. Phys*. **1995**, *102*, 754.
(9) Schwarz, J.; Heinemann, C.; Schwarz, H. *J. Phys. Chem*. **1995**, *99*, 11405.
(10) Asher, R. L.; Bellert, D.; Buthelezi, T.; Brucat, P. J. *Chem. Phys. Lett*. **1994**, *227*, 623.
(11) Baranov, V.; Javahery, G.; Hophinson, A. C.; Bohme, D. K. *J. Am. Chem. Soc*. **1995**, *117*, 12801.
(12) Jeung, G. *Mol. Phys*. **1989**, *67*, 747.
(13) Caballol, R.; Sanchez Marcos, E.; Barthelat, J. C. *J. Phys. Chem*. **1987**, *91*, 1328.
(14) Sodupe, M.; Branchadell, V.; Oliva, A. *J. Phys. Chem*. **1995**, *99*, 8567.
(15) Sodupe, M.; Branchadell, V.; Oliva, A. *J. Mol. Struct*. **1996**, *371*, 79.
(16) Sodupe, M.; Branchadell, V.; Rosi, M.; Bauchlicher, C. W., Jr. *J. Phys. Chem. A* **1997**, *101*, 1854.
(17) Chertihin, G. V.; Andrews, L. *J. Am. Chem. Soc*. **1995**, *117*, 1595.
(18) Souter, P. F.; Andrews, L. *J. Am. Chem. Soc*. **1997**, *119*, 7350.
(19) Burkholder, T. R.; Andrews, L. *J. Chem. Phys*. **1991**, *95*, 8697; Hassanzadeh, P.; Andrews, L. *J. Phys. Chem*. **1992**, *96*, 9177.

10.1021/ja982900+ CCC: $15.00
Published on Web 11/26/1998

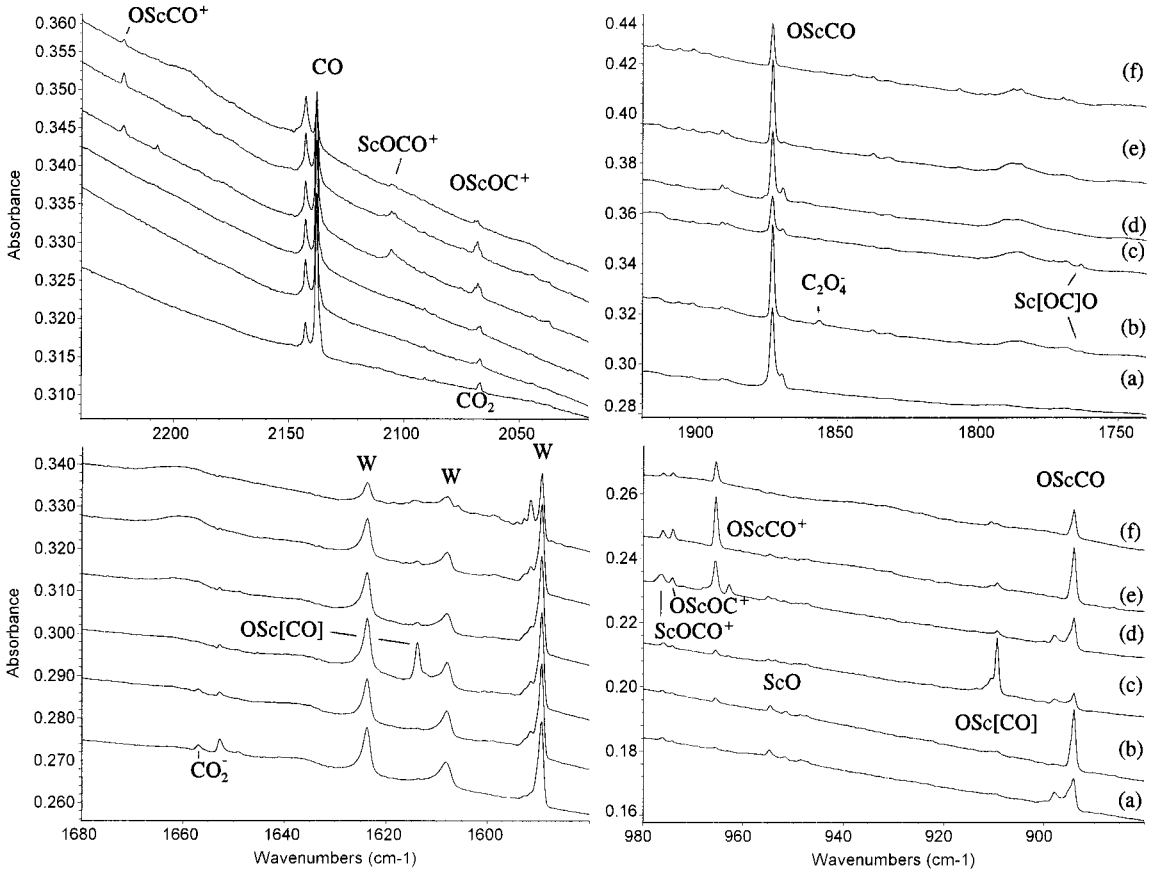

Figure 1. Infrared spectra in selected regions for reaction of laser-ablated Sc atoms with 0.5% CO_2 in excess argon during condensation at 12 K: (a) sample co-deposition for 1 h, (b) after annealing to 25 K, (c) after $\lambda > 470$ nm photolysis, (d) after full arc photolysis, (e) after annealing to 30 K, and (f) after annealing to 35 K. W denotes trace water impurity.

and a very weak combination band at 2067.0 cm^{-1}.[20] The spectra of laser-ablated Sc atoms codeposited with 0.5% CO_2 in excess argon in selected regions are shown in Figure 1, and the absorptions are listed in Table 1. After deposition, two strong bands at 1873.4 and 894.1 cm^{-1} were observed together with CO absorption at 2138.3 cm^{-1} and weak absorptions at 976.2 and 954.8 cm^{-1} previously assigned to ScO.[21] The strong 1873.4 and 894.1 cm^{-1} and two very weak 1763.4 and 778.0 cm^{-1} absorptions increased together on 25K annealing. Mercury arc photolysis with a 470-nm long-wavelength pass filter (essentially 546- and 578-nm mercury emissions) almost destroyed the two strong bands, produced two other bands at 1613.9 and 909.6 cm^{-1}, and further increased the latter very weak bands. Another photolysis using the mercury arc lamp without a filter destroyed the 1613.9, 909.6 cm^{-1} and 1763.4, 778.0 cm^{-1} bands, almost recovered the 1873.4 and 894.1 cm^{-1} bands, and produced three new band sets at 965.5, 2221.8 cm^{-1}, 976.4, 2105.7 cm^{-1}, and 974.1, 2068.1 cm^{-1} (on top of the very weak CO_2 band at 2067.0 cm^{-1}). Further annealing to 30 K decreased the 894.1, 965.5, 974.1, 1873.4, 2068.1, 2105.7, and 2221.8 cm^{-1} bands.

Another experiment was done to explore the photochemistry more thoroughly, and the lower frequency region, which contains one member of each band pair, is shown in Figure 2. Again annealing to 25 K approximately doubled the strong 894.1, 1873.4 cm^{-1}, weak 965.5, 2221.8 cm^{-1}, and very weak 778.0, 1763.4 cm^{-1} band pairs with little effect on other absorptions. Photolysis with $\lambda > 630$ nm using a tungsten lamp markedly increased the 909.6, 1613.9 cm^{-1} bands at the expense of the strong 894.1, 1873.4 cm^{-1} pair (Figure 2c), and $\lambda > 470$ nm photolysis with the Hg arc continued this trend (Figure 2d). Additional photolysis $\lambda > 380$ nm reversed this trend and promoted the 778.0, 1763.4 cm^{-1} pair (Figure 2(e)), but irradiation $\lambda > 290$ nm destroyed the latter pair, further decreased the 909.6, 1613.9 cm^{-1} set, and increased the strong 894.1, 1873.4 cm^{-1} pair to almost double their original absorbances (Figure 2f). Full arc photolysis slightly decreased the latter bands and increased 965.5, 2221.8 cm^{-1} bands 4-fold and 974.1, 976.4, 2068.1, and 2105.7 cm^{-1} bands about 50% (Figure 2g). A final second $\lambda > 470$ nm irradiation halved the strong 894.1, 1873.4 cm^{-1} pair and increased the 909.6, 1613.9 cm^{-1} pair 4-fold (Figure 2h), similar to the first exposure to $\lambda > 470$ nm radiation.

A weak band at 1657.0 cm^{-1} decreased by annealing and destroyed by photolysis is due to the CO_2^- anion isolated in solid argon, in agreement with the 1658.3 cm^{-1} solid neon assignment.[22] The sharp, weak 1856.7 and 1184.7 cm^{-1} bands produced on annealing and destroyed by photolysis, also observed with different metal targets, are due to $C_2O_4^-$ as will be discussed fully in a later report.[23] Weak 1891.5, 1257.0 and 691.2 cm^{-1} bands are due to CO_4^-.[22,23]

Similar spectra were obtained using isotopic $^{13}C^{16}O_2$ and $^{12}C^{18}O_2$ samples. No isotopic shifts were observed for bands in the 1000−880 cm^{-1} region in the $^{13}C^{16}O_2$ experiment, while the 1613.9, 1873.4, 2067.0, and 2221.8 cm^{-1} bands shifted to

(20) Andrews, L.; Arlinghaus, R. T.; Johnson, G. L. *J. Chem. Phys.* **1983**, *78*, 6353; Herzberg, G. *Infrared and Raman Spectra*; Van Nostrand: New York, 1945.

(21) Chertihin, G. V.; Andrews, L.; Rosi, M.; Bauschlicher, C. W., Jr. *J. Phys. Chem. A* **1997**, *101*, 9085. The 976.2 cm^{-1} band will be reassigned to ScO^+ in a future report.

(22) Jacox, M. E.; Thompson, W. E. *J. Chem. Phys.* **1989**, *91*, 1410; *J. Phys. Chem.* **1991**, *95*, 2781.

Table 1. Infrared Absorptions (cm^{-1}) from Codeposition of Laser-Ablated Sc Atoms and Electrons with CO_2 Molecules in Excess Argon at 10 K

$^{12}C^{16}O_2$	$^{13}C^{16}O_2$	$^{12}C^{18}O_2$	$^{12}C^{16}O_2 + {}^{13}C^{16}O_2$	$C^{16}O_2 + C^{16,18}O_2 + C^{18}O_2$	*R*(12/13)	*R*(16/18)	assign
2344.8	2279.2	2309.7	2344.8,2279.2	2344.8, 2327.8, 2309.7	1.02878	1.01520	CO_2
2339.0	2273.6	2304.1	2339.0, 2273.6	2339.0, 2322.0, 2304.1	1.02876	1.01515	CO_2
2221.8	2172.1	2169.9	2221.8, 2172.1	2221.7, 2169.9	1.02288	1.02392	$OScCO^+$
2207.2	2158.1		2207.2, 2158.1		1.02275		site
2143.0	2095.7	2092.0	2143.0, 2095.7	2143.0, 2092.0	1.02257	1.02438	$(CO)_x$
2138.2	2091.2	2087.3	2138.2, 2091.2	2138.2, 2087.3	1.02248	1.02439	CO
2105.7	2059.4	2055.4	2105.6, 2059.4	2105.6, 2055.4	1.02248	1.02247	$ScOCO^+$
2068.1	2022.9	2018.8	2068.1, 2022.9	2068.1, 2018.8	1.02234	1.02442	$OScOC^+$
2067.0	2029.0	2012.3			1.01873	1.02718	CO_2
1891.5	1831.5	1863.3	1891.5, 1831.5		1.03276	1.01513	CO_4^-
1873.4	1830.6	1831.7	1873.4, 1830.5	1873.4, 1831.7	1.02338	1.02277	OScCO
1856.7	1806.4	1826.8	1856.9, 1806.7	1856.4, 1842.0, 1826.8	1.02785	1.01637	$C_2O_4^-$
1763.4	1721.4	1729.7	1763.4, 1721.4	1763, 1729.7	1.02440	1.01948	Sc[OC]O
1657.0	1612.9	1629.3	1657.0, 1612.9	1657.0, 1643.9, 1629.3	1.02734	1.01700	CO_2^- site
1652.7	1608.8	1625.0	1652.7, 1608.8	1652.7, 1639.8, 1625.0	1.02729	1.01705	$(CO_2^-)(CO_2)_x$
1613.9	1578.7	1575.3	1613.8, 1578.7	1613.9, 1575.3	1.02230	1.02450	OSc[CO]
1383.9	1368.3	1339.2	1383.8, 1368.6	1383.9, 1359.4, 1339.3	1.01140	1.03338	$(CO_2)_x$
1279.0	1255.9	1227.7	1278.3, 1256.0	1278.4, 1254.6, 1227.7	1.01839	1.04179	$(CO_2)_x$
1274.0	1264.8	1221.7	1273.8, 1268.3, 1264.7		1.00727	1.04281	?
1257.0	1248.2	1200.2			1.00705	1.04733	CO_4^-
1249.1	1240.6	1192.4			1.00685	1.04755	site
1184.7	1177.3	1130.5	1184.6, 1180.6, 1177.0	1168.3, 1157.1, 1148.4, 1141.3	1.00629	1.04794	$C_2O_4^-$
976.4	976.4	935.5	976.4	976.4, 935.5		1.04372	$ScOCO^+$
976.2	976.2	935.3	976.2	976.2, 935.3		1.04373	ScO^+
974.1	974.1	933.5	974.1	974.2, 933.5		1.04349	$OScOC^+$
965.5	965.5	925.2	965.5	965.6, 925.2		1.04356	$OScCO^+$
962.8	962.8		962.8				$OScOC^+$ site
954.8	954.8	915.0	954.8	954.8, 915.0		1.04350	ScO
951.8	951.7	912.0	951.8			1.04364	ScO site
909.6	909.6	871.9	909.6	909.6, 871.9		1.04324	OSc[CO]
898.0	897.9	860.6		897.9, 860.6		1.04346	OScCOsite
894.1	894.1	857.2	894.1	894.2, 857.2		1.04305	OScCO
778.0	770.8	748.9			1.00934	1.03886	Sc[OC]O
691.2	681.0		691.1, 681.0	691.2, 680.8	1.01498		CO_4^-
663.5	644.6	653.5		663.5, 658.5, 653.5	1.02930	1.01530	CO_2
661.9	643.2	651.9		661.9, 656.9, 651.9			CO_2

1578.7, 1830.6, 2029.0, and 2172.1 cm^{-1}, respectively. In the $^{12}C^{18}O_2$ experiment, all of these product absorptions exhibited isotopic shifts as listed in Table 1. For band identification, mixed $^{12}C^{16}O_2 + {}^{13}C^{16}O_2$ and $^{12}C^{16}O_2 + {}^{12}C^{16,18}O_2 + {}^{12}C^{18}O_2$ experiments were also done; all metal product absorptions exhibited doublet isotopic structures as shown in Figures 3 and 4.

Y + CO_2/Ar. The spectra of laser ablated Y atoms codeposited with 0.5% CO_2 in argon are shown in Figure 5, and the absorptions are listed in Table 2. Similar with the Sc + CO_2 reaction, strong absorptions at 1861.5 and 796.5 cm^{-1} and weak YO^+ and YO absorptions at 871.9 and 843.0 cm^{-1} were observed on deposition.[24] The 1861.5 and 796.5 cm^{-1} bands increased about 50% on 25 K annealing. Mercury arc photolysis with the 470-nm long-wavelength pass filter decreased these two bands by 80% and produced two other bands at 1614.5 and 804.4 cm^{-1}. Another photolysis using the mercury arc without filter destroyed the 1614.5 and 804.4 cm^{-1} bands, decreased the 796.5 and 1861.5 cm^{-1} bands by 60%, and produced strong new bands at 857.2, and 2206.0, 2203.3 cm^{-1} and weak new absorptions at 869.1, 871.9 (on top of YO^+), 2078.0, and 2106.0 cm^{-1}. Again, isotopic experiments were done for band identification, and the results are also listed in Table 2.

Calculations. Density functional calculations were performed for the product molecules expected here using the Gaussian 94 program.[25] Due to the similarity of Sc and Y, calculations were only performed on the Sc product system. The BP86 as well as the B3LYP functionals,[26−28] the 6-311+G* basis sets for C and O atoms, and the set of Wachters and Hay for Sc were used.[29,30] Four $ScCO_2$ isomers were calculated, namely OSc-CO, OSc-(η^2-CO), Sc-(η^2-OC)O, and Sc-(η^2-OO)C. The ScOCO and Sc-CO_2 isomers were calculated earlier[14] to be higher in energy than Sc-(η^2-OC)O and Sc-(η^2-OO)C and are not listed here. The inserted OScCO molecule was calculated to be the most stable, followed by the new OSc-(η^2-CO) molecule, which was only 6.4 kcal/mol (BP86) or 5.0 kcal/mol (B3LYP) higher than the OScCO molecule. The Sc-(η^2-OC)O and Sc-(η^2-OO)C isomers were calculated about 12−15 kcal/mol higher than OScCO, as listed in Table 3. These results are in reasonable agreement with calculations reported by Sodupe et al.,[14,15] who also found OScCO to be the most stable, and the Sc-(η^2-OC)O and Sc-(η^2-OO)C isomers about 17 kcal/mol higher, but they did not

(23) Zhou, M. F.; Andrews, L., *J. Chem. Phys.*, in press.

(24) Chertihin, G. V.; Zhou, M. F.; Bare, W. D.; Andrews, L. To be submitted (Y + O_2).

(25) *Gaussian 94, Revision B.1*: Frisch, M. J.; Trucks, G. W.; Schlegel, H. B.; Gill, P. M. W.; Johnson, B. G.; Robb, M. A.; Cheeseman, J. R.; Keith, T.; Petersson, G. A.; Montgomery, J. A.; Raghavachari, K.; Al-Laham, M. A.; Zakrzewski, V. G.; Ortiz, J. V.; Foresman, J. B.; Cioslowski, J.; Stefanov, B. B.; Nanayakkara, A.; Challacombe, M.; Peng, C. Y.; Ayala, P. Y.; Chen, W.; Wong, M. W.; Andres, J. L.; Replogle, E. S.; Gomperts, R.; Martin, R. L.; Fox, D. J.; Binkley, J. S.; Defrees, D. J.; Baker, J.; Stewart, J. P.; Head-Gordon, M.; Gonzalez, C.; Pople, J. A. Gaussian, Inc., Pittsburgh, PA, 1995.

(26) Lee, C.; Yang, E.; Par, R. G. *Phys. Rev. B* **1988**, *37*, 785.

(27) Perdew, J. P. *Phys. Rev. B* **1986**, *33*, 8822.

(28) Becke, A. D. *J. Chem. Phys.* **1993**, *98*, 5648.

(29) McLean, A. D.; Chandler, G. S. J. Chem. Phys. **1980**, *72*, 5639. Krishnan, R.; Binkley, J. S.; Seeger, R.; Pople, J. A. *J. Chem. Phys*. **1980**, *72*, 650.

(30) Wachters, J. H.; *J. Chem. Phys*. **1970**, *52*, 1033; Hay, P. J. *J. Chem. Phys*. **1977**, *66*, 4377.

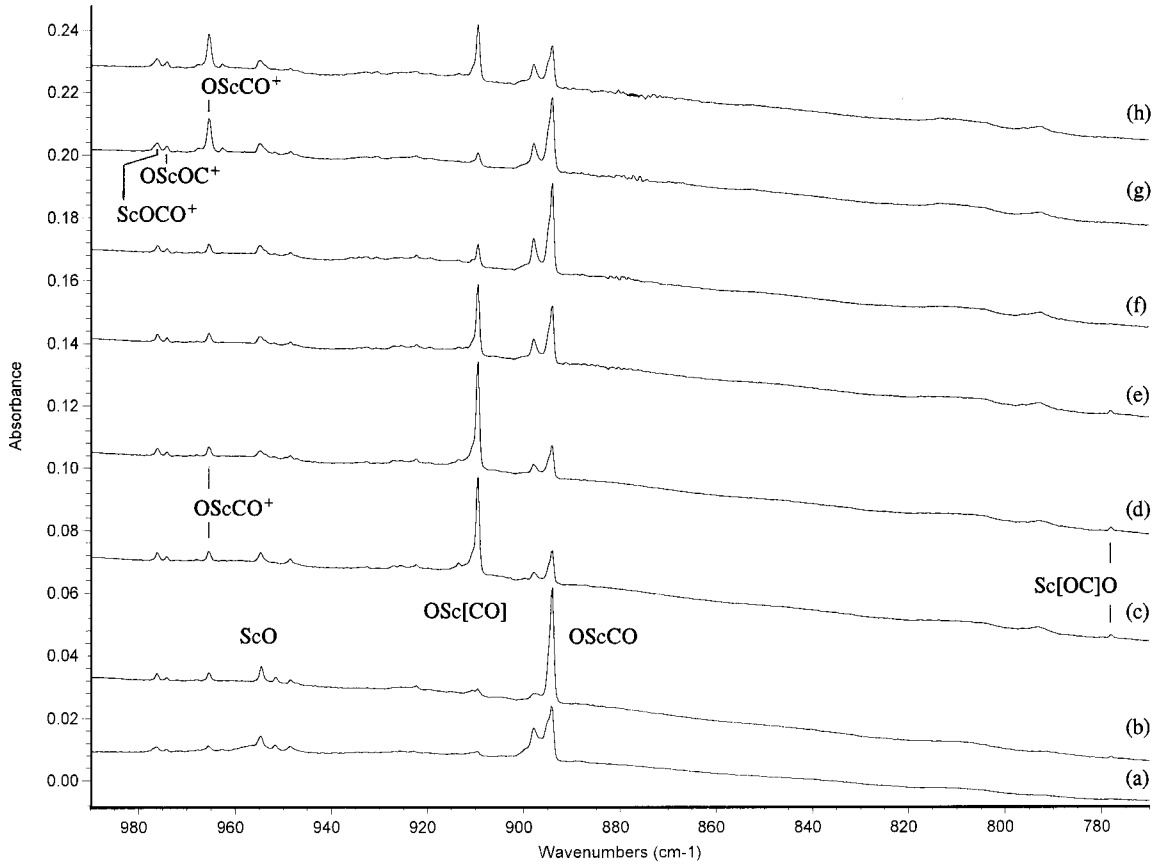

Figure 2. Infrared spectra in the low-frequency region for reaction of laser-ablated Sc atoms with 0.5% CO_2 in excess argon during condensation at 12 K: (a) sample co-deposition for 1 h, (b) after annealing to 25 K, (c) after $\lambda > 630$ nm photolysis from 500-W tungsten lamp, (d) after $\lambda > 470$ nm photolysis from a 175-W mercury arc, (e) after $\lambda > 380$ nm photolysis, (f) after $\lambda > 290$ nm photolysis, (g) after full arc $240 < \lambda < 580$ nm photolysis, and (h) after second $\lambda > 470$ nm photolysis.

investigate the OSc-(η^2-CO) isomer. The calculated frequencies (not scaled) for $ScCO_2$ isomers described in Table 3 are listed in Table 4.

Similar calculations were also done for the $OScCO^+$ molecular cation and the more weakly bound $OScOC^+$, $ScOCO^+$, and $ScOOC^+$ isomers, and the results are listed in Table 3. The $^3\Delta$ state of Sc^+OCO calculated earlier[16] is essentially perturbed OCO and is 18.4 kcal/mol above the $^1\Sigma^+$ state of ScO^+CO reported here. Table 5 lists the observed and calculated isotopic frequency ratios for the Sc−O and C−O stretching fundamentals of the OScCO, OSc-(η^2-CO), Sc-(η^2-OC)O neutral and OScCO$^+$, $OScOC^+$, $ScOCO^+$ cation species.

The $^3A''$ anion $OScCO^-$ was also calculated, and results are listed in Tables 3−5.

Discussion

Six new product molecules and cations will be identified from isotopic shifts and DFT calculations of isotopic frequencies.

OScCO. The 1873.4 and 894.1 cm^{-1} bands were the dominant absorptions on deposition. These two bands tracked throughout all the experiments, suggesting that they are due to different vibrational modes of the same molecule. The 894.1 cm^{-1} band showed no carbon-13 isotopic shift, but shifted to 857.2 cm^{-1} using the $C^{18}O_2$ sample; the 16/18 isotopic ratio (1.04305) is slightly lower than this ratio for the diatomic molecule ScO, and the frequency is also slightly lower than diatomic ScO frequency in solid argon.[21] The doublet with mixed isotopic oxygen verifies that a single O atom is involved. This confirms that the 894.1 cm^{-1} band is also due to a terminal Sc−O stretching vibration.

The 1873.4 cm^{-1} band shifts to 1830.6 cm^{-1} using the $^{13}C^{16}O_2$ sample and to 1831.7 cm^{-1} using the $^{12}C^{18}O_2$ reagent; the 12/13 isotopic ratio (1.02338) and 16/18 ratio (1.02277) indicate that this is a C−O stretching vibration. This band is 264.9 cm^{-1} lower than the diatomic CO frequency in solid argon. Note that these ratios are slightly higher and lower, respectively, than the diatomic C−O values. This shows that C is moving more and O less than in the CO diatomic molecule and suggests bonding of another atom to carbon such that the vibration of carbon is "pseudoantisymmetric" between the other atom and oxygen. The doublet structure in both mixed $^{12}C^{16}O_2 + {}^{13}C^{16}O_2$ and $^{12}C^{16}O_2 + {}^{12}C^{16,18}O_2 + {}^{12}C^{18}O_2$ experiments confirms that only one CO subunit is involved in this mode. Similar to the Ti and Cr systems,[17,18] these two bands are suitable for assignment to the inserted OScCO molecule.

This assignment is in excellent agreement with DFT calculations. The OScCO molecule has a $^2A''$ ground state, with a O−Sc−C angle of 110°. The BP86 calculation gave 917.4 cm^{-1} Sc−O and 1912.7 cm^{-1} C−O stretching frequencies, which must be multiplied by 0.975 and 0.979 to reproduce the observed frequencies, while the B3LYP calculation gave slightly higher values (945.0 and 1975.8 cm^{-1}). This is in accord with the expected accuracy of DFT calculations.[31] Agreement between BP86 and B3LYP calculations indicates that OScCO is well defined by DFT. The calculated isotopic ratios also match the observed values; both BP86 and B3LYP calculations predicted no carbon isotopic shift for the Sc−O stretching mode and isotopic ratios for the C−O mode, in excellent agreement with observations (Table 5). The calculated relative intensities for the C−O and Sc−O stretching modes (BP86, 559/252; B3LYP,

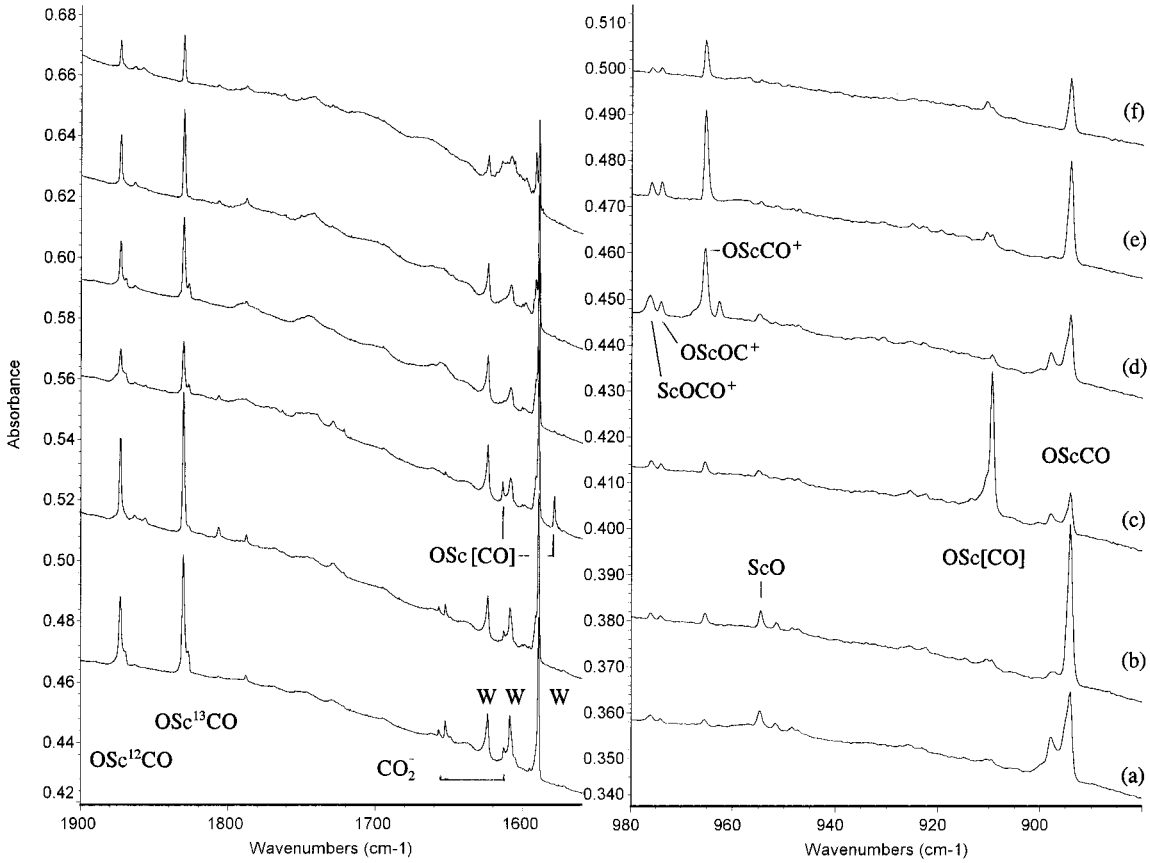

Figure 3. Infrared spectra in selected regions for reaction of laser-ablated Sc atoms with 0.4% $^{12}CO_2$ + 0.6% $^{13}CO_2$ in excess argon during condensation at 12 K: (a) sample co-deposition for 1 h, (b) after annealing to 25 K, (c) after $\lambda > 470$ nm photolysis, (d) after full arc photolysis, (e) after annealing to 30 K, and (f) after annealing to 35 K. W denotes trace water impurity.

798/374) are also in very good agreement with experimental value (0.0371/0.0187). This means that the observed molecule and normal modes are correctly characterized by the DFT calculations.

OYCO. Similar absorptions at 1861.5 and 796.5 cm^{-1} in the Y + CO_2 reaction can be assigned to C−O and Y−O stretching vibrations of the OYCO molecule. The 1861.5 cm^{-1} band exhibited C−O stretching isotopic ratios (12/13, 1.02331; 16/18, 1.02308), the doublet mixed isotopic structure confirms that only one CO subunit is involved. Again, the 796.5 cm^{-1} band showed no carbon isotopic shift and a slightly lower diatomic 16/18 ratio (1.05065) than the YO molecule.[24]

OSc-(η^2-CO) or OSc[CO]. The 1613.9 and 909.6 cm^{-1} bands appeared on mercury arc photolysis with the 470-nm long-wavelength pass filter, and full arc photolysis destroyed these two bands. The 1613.9 cm^{-1} band shifted to 1578.7 and 1575.3 cm^{-1} using the $^{13}C^{16}O_2$ and $^{12}C^{18}O_2$ reagents, the 12/13 ratio (1.02230) and 16/18 ratio (1.02450) indicate that this band is an almost pure diatomic C−O stretching vibration, but the frequency is 524.4 cm^{-1} lower than the diatomic CO frequency, indicating that this is not a terminal C−O stretching vibration. In analogous Sc + N_2 and Sc + NO reactions,[32,33] the side-bonded M[N_2] and M[NO] molecules also show large red shifts corresponding to the end-bonded molecules. So a side-bonded structure must be considered. In the mixed $^{12}C^{16}O_2$ + $^{13}C^{16}O_2$ and $^{12}C^{16}O_2$ + $^{12}C^{16,18}O_2$ + $^{12}C^{18}O_2$ experiments, only pure isotopic counterparts were observed, so one CO subunit is involved in this vibration. The associated 909.6 cm^{-1} band showed no carbon isotopic shift, the 16/18 ratio (1.04324) characterized this vibration as a terminal Sc−O stretching vibration, and the doublet structure in $^{12}C^{16}O_2$ + $^{12}C^{16,18}O_2$ + $^{12}C^{18}O_2$ experiment confirmed the involvement of only one O atom. Because these two bands were produced on photolysis when the OScCO molecular absorptions were destroyed, the side-bonded OSc-(η^2-CO) isomer is suggested for consideration.

The OSc-(η^2-CO) structure was confirmed by DFT calculations reported here. Both BP86 and B3LYP calculations predict that the OSc-(η^2-CO) molecule has a $^2A'$ ground state and is only 6.4 kcal/mol (BP86) or 5.0 kcal/mol (B3LYP) higher in energy than the insertion OScCO molecule, but lower than other $ScCO_2$ isomers. The C−O stretching frequency was calculated to be 1648.6 cm^{-1} by BP86 and 1688.5 cm^{-1} by B3LYP, very close to the 1613.9 cm^{-1} value observed. The Sc−O stretching frequency was calculated to be 929.3 cm^{-1} by BP86 and 959.1 cm^{-1} by B3LYP, again just above the 909.6 cm^{-1} observed value. Note the calculated isotopic ratios as listed in Table 5 are in excellent agreement with experimental values.

OY-(η^2-CO) or OY[CO]. Similar bands at 1614.5 and 804.4 cm^{-1} in the Y + CO_2 system were also produced together on mercury arc photolysis using the 470-nm long-wavelength pass filter and destroyed on full arc photolysis. The 1614.5 cm^{-1} band shifted to 1579.2 cm^{-1} and 1576.0 cm^{-1} in $^{13}C^{16}O_2$ and $^{12}C^{18}O_2$ experiments. The 804.4 cm^{-1} band exhibited no carbon isotopic shift but shifted to 765.6 cm^{-1} using $^{12}C^{18}O_2$ sample. The doublet structure in mixed experiments confirmed only one CO molecule in the upper mode and one O atom involved in

(31) Scott, A. P.; Radom, L. *J. Phys. Chem.* **1996**, *100*, 16502.
(32) Chertihin, G. V.; Andrews, L.; Bauschlicher, C. W., Jr. *J. Am. Chem. Soc.* **1998**, *120*, 3205.
(33) Kushto, G. P.; Zhou, M. F.; Andrews, L.; Bauschlicher, C. W., Jr., submitted (Sc, Ti + NO).

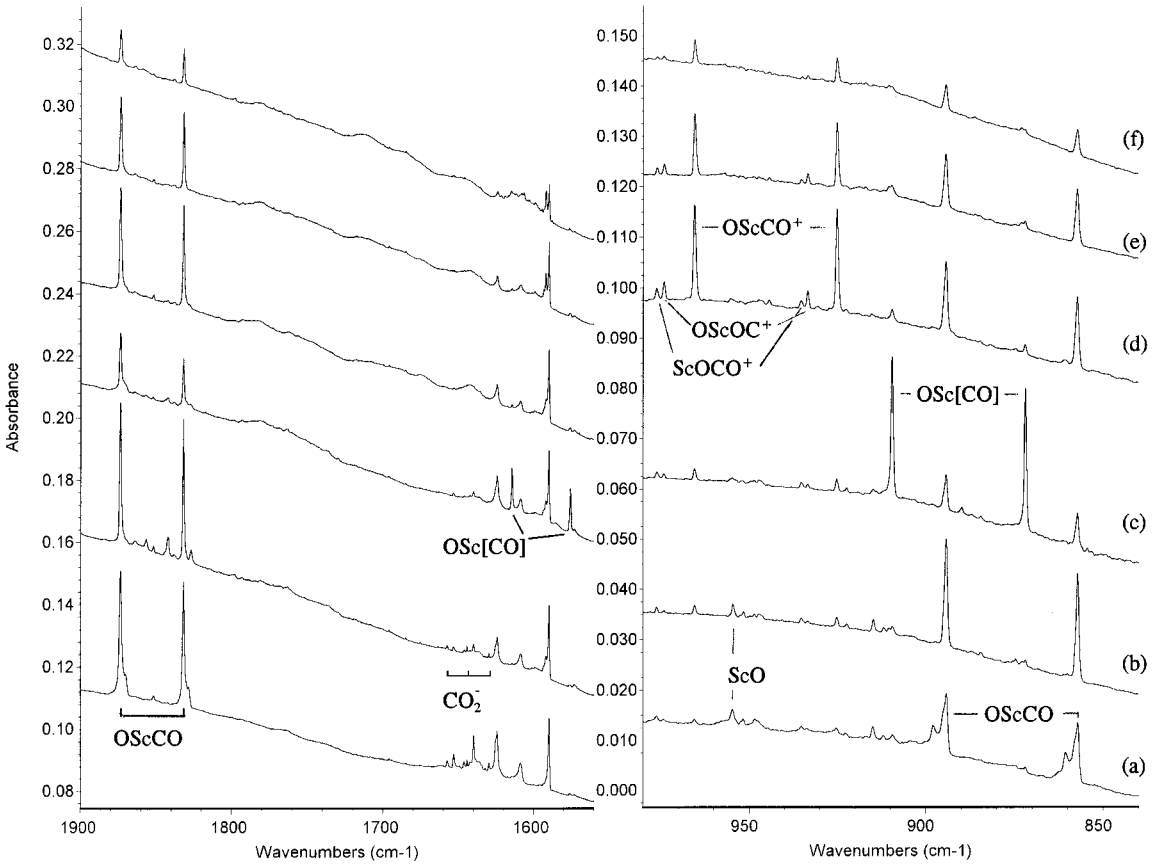

Figure 4. Infrared spectra in selected regions for reaction of laser-ablated Sc atoms with 0.5% statistical $C^{16}O_2 + C^{16,18}O_2 + C^{18}O_2$ in excess argon during condensation at 12 K: (a) sample co-deposition for 1 h, (b) after annealing to 25 K, (c) after $\lambda > 470$ nm photolysis, (d) after full arc photolysis, (e) after annealing to 30 K, and (f) after annealing to 35 K.

the lower mode. Accordingly, these two bands are assigned to C−O stretching and Y−O stretching vibrations of the OY-(η^2-CO) molecule following the example of OSc-(η^2-CO).

Sc-(η^2-OC)O or Sc[OC]O. The very weak 778.0 and 1763.5 cm^{-1} bands increase on 25 K annealing and photolysis through $\lambda > 380$ nm but are destroyed with $290 < \lambda < 380$ nm radiation. These are the lowest bands in each region, and their isotopic ratios are unusual. The 778.0 cm^{-1} band shows a 7.2 cm^{-1} carbon-13 shift in contrast to the 0.0 cm^{-1} carbon-13 shift of the other low-frequency bands, and the 29.1 cm^{-1} oxygen-18 shift is correspondingly less. This indicates a Sc[OC] ring stretching mode involving both carbon *and* oxygen. The 1763.4 cm^{-1} band exhibits a much larger carbon-13 shift (42.0 cm^{-1}) than oxygen-18 (33.7 cm^{-1}) shift, which shows that this motion retains some antisymmetric O−C−O stretching character.

DFT calculations for the most stable addition product, bridged Sc-(η^2-OC)O, provide frequencies at 829.5 and 1761.8 cm^{-1} with calculated 12/13 and 16/18 ratios in good agreement with the unusual experimental values (Table 5). This agreement in frequency position and isotopic ratios supports the identification of the Sc-(η^2-OC)O addition product. Although the $OScCO^-$ anion is predicted to absorb near 1800 cm^{-1}, the normal modes of this open species are quite different, and the $OScCO^-$ anion cannot be identified here.

The 1773.1 cm^{-1} band for Y behaved similarly, gave a 1773.1, 1731.6 cm^{-1} doublet with $^{12,13}CO_2$, and can be assigned to Y[OC]O.

$OScCO^+$. The 2221.8 and 965.5 cm^{-1} bands increased markedly on full arc photolysis and decreased together on subsequent 30 and 35 K annealing. The 2221.8 cm^{-1} band shifted to 2172.1 and 2169.9 cm^{-1} using $^{13}C^{16}O_2$ and $^{12}C^{18}O_2$ reagents. The isotopic 12/13 ratio (1.02288) and 16/18 ratio (1.02392) are very close to the diatomic CO ratios. Both mixed $^{12}C^{16}O_2 + {}^{13}C^{16}O_2$ and $^{12}C^{16}O_2 + {}^{12}C^{16,18}O_2 + {}^{12}C^{18}O_2$ experiments gave doublet isotopic structures, indicating that this band is due to a single C−O molecule stretching vibration. The associated 965.5 cm^{-1} band also shows no carbon isotopic shift like the OScCO molecule, and the 1.04356 isotopic ratio indicates that this is a terminal Sc−O stretching vibration. Furthermore, the doublet in the mixed $^{12}C^{16}O_2 + {}^{12}C^{16,18}O_2 + {}^{12}C^{18}O_2$ sample confirms that only one O atom is involved. So this new species also has the $ScCO_2$ stoichiometry.

However, these two bands do not fit any known $ScCO_2$ isomers. Note that the 2221.8 cm^{-1} band is 348.4 cm^{-1} *higher* than the C−O stretching frequency of the OScCO molecule, and even 83.5 cm^{-1} *higher* than the CO molecule! So the $OScCO^+$ cation comes to mind. Previous DFT/B3LYP calculations[16] on the interaction of Sc^+ with CO_2 find that the $OScCO^+$ structure is more stable than the $ScOCO^+$ arrangement. Because of the very strong MO^+ bond formed, the $OScCO^+$ cation is 50.3 kcal/mol below the ground-state $Sc^+ + CO_2$ asymptote, but in that paper, no C−O and Sc−O stretching vibrational frequencies were reported.[16] Our DFT calculations obtained a very similar optimized $OScCO^+$ geometry. The C−O stretching frequency was calculated with BP86 at 2210.6 cm^{-1}, slightly lower than the observed 2221.8 cm^{-1} value, while the B3LYP calculation gave 2312.6 cm^{-1}, somewhat higher than 2221.8 cm^{-1} value. The Sc−O stretching frequency was calculated at 1009.9 and 1052.6 cm^{-1} for the two methods. Again, the calculated isotopic ratios for both vibrational modes are in excellent agreement with the observed values as listed in Table 5. Note that the 12/13 isotopic ratio is only slightly higher than

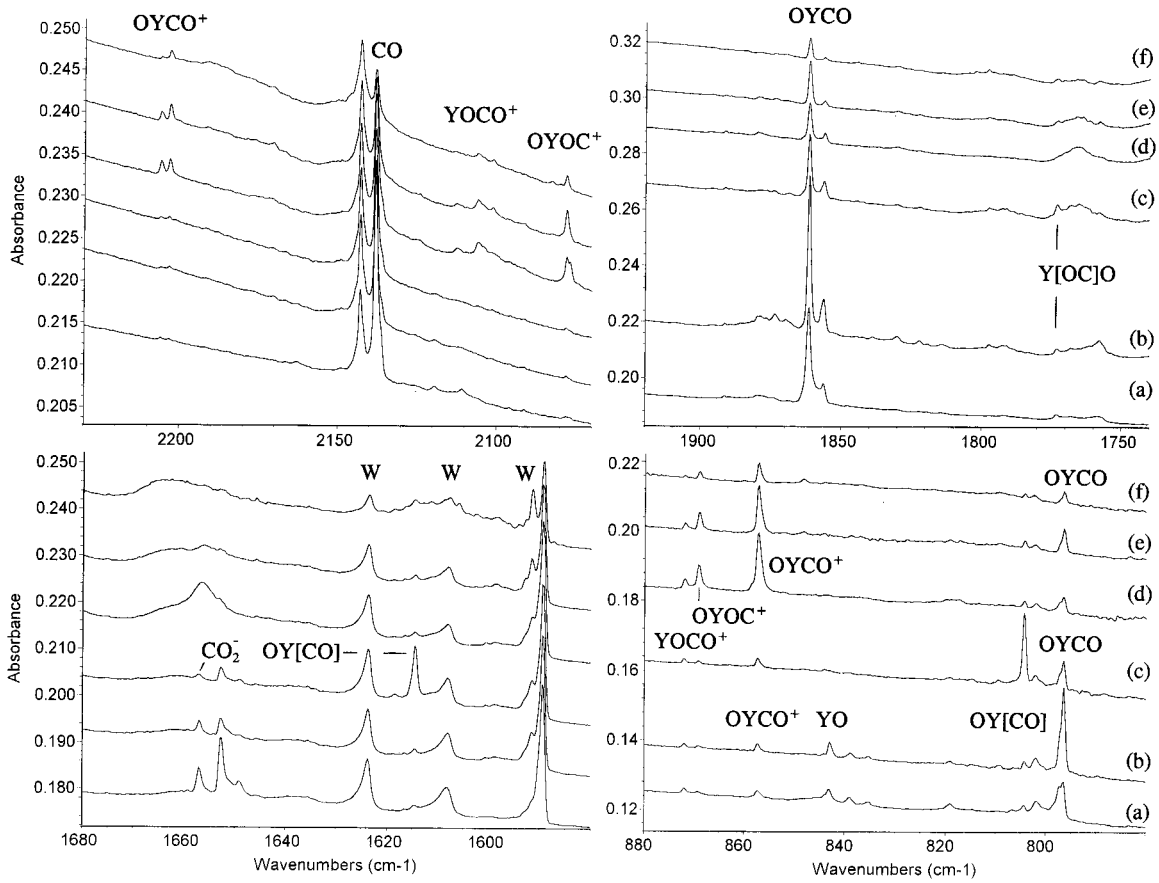

Figure 5. Infrared spectra in selected regions for reaction of laser-ablated Y atoms with 0.5% CO_2 in excess argon during condensation at 12 K: (a) sample co-deposition for 1 h, (b) after annealing to 25 K, (c) after $\lambda > 470$ nm photolysis, (d) after full arc photolysis, (e) after annealing to 30 K, and (f) after annealing to 35 K. W denotes trace water impurity.

Table 2. Infrared Absorptions (cm^{-1}) from Reaction of Laser-Ablated Y Atoms with CO_2 Molecules in Excess Argon at 10 K

$^{12}C^{16}O_2$	$^{13}C^{16}O_2$	$^{12}C^{18}O_2$	*R*(12/13)	R(16/18)	assign
2206.0	2156.8	2154.2	1.02281	1.02405	$OYCO^+$
2203.3	2154.1	2151.4	1.02284	1.02412	$OYCO^+$ site
2143.0	2095.7	2092.0	1.02257	1.02438	$(CO)_x$
2138.2	2091.2	2087.3	1.02248	1.02439	CO
2106.0	2059.7	2055.9	1.02248	1.02437	YO^+CO
2078.0	2032.3	2028.4	1.02249	1.02445	OY^+OC
1861.5	1819.1	1819.5	1.02331	1.02308	OYCO
1856.1	1814.1	1814.3	1.02315	1.02304	OYCO site
1773.1	1731.6		1.02397		Y[OC]O
1614.5	1579.2	1576.0	1.02235	1.02443	OY[CO]
871.9	871.9	829.9		1.05061	YO^+, $YOCO^+$
869.1	869.1	827.3		1.05053	$OYOC^+$
857.2	857.2	816.0		1.05049	$OYCO^+$
843.0					YO
838.9					YO
835.5					YO
819.0	819.0	779.9		1.05013	?
804.4	804.4	765.6		1.05068	OY[CO]
802.0	802.0	763.3		1.05070	OYCO site
796.5	796.5	758.1		1.05065	OYCO

the diatomic value, indicating very little mechanical effect of carbon bonding to Sc in accord with the much longer Sc−C bond length in the cation as compared to the neutral OScCO case. Unlike the two neutral molecules OScCO and OSc-(η^2-CO) observed here, where the C−O stretching vibration was more intense than the Sc−O stretching vibration, the observed C−O stretching vibration was weaker than the Sc−O stretching mode for the $OScCO^+$ cation, as the calculations also predict.

Weak nearby bands at 2207.2 and 962.9 cm^{-1}, also produced together on photolysis, had isotopic behaviors similar to those of the 2221.8 and 965.5 cm^{-1} bands. These bands are assigned to $OScCO^+$ cations with different matrix environments. Note that 30 K annealing increases the former at the expense of the latter matrix site bands.

$OYCO^+$. Similar bands at 2206.0, 2203.3 and 857.2 cm^{-1} in the Y + CO_2 system exhibit analogous annealing and photochemical behavior as $OScCO^+$ cations and are assigned to $OYCO^+$ cations at different sites.

$OScOC^+$ and $ScOCO^+$. Two other weak bands are produced on full arc photolysis at 2105.7 and 2068.1 cm^{-1}, just below the CO absorption at 2138.2 cm^{-1}, and decrease on 30 and 35 K annealing. These bands give doublet absorptions in both mixed isotopic experiments and 12/13 and 16/18 isotopic ratios extremely close to CO itself, so both absorptions are due to CO with a very weak interaction. Two weak bands at 976.4 and 974.1 cm^{-1} track, respectively, with the above bands on annealing and photolysis, and the broader pair at 2105.7 and 976.4 cm^{-1} decreases more on 30 K annealing than the sharper pair at 2068.1 and 974.1 cm^{-1}.

The isoelectronic OBeCO and OBeOC molecules have been observed,[34] and their frequencies have the same relationship as $OScCO^+$ and $OScOC^+$, respectively. The OSc^+ cation is clearly a stronger Lewis acid than the OBe molecule, and the C−O fundamental in $OScCO^+$ (2221.8 cm^{-1}) is higher than that for OBeCO (2189.5 cm^{-1}).

Our DFT calculations show that two more cation species, essentially ScO^+ electrostatically bound to CO, are less stable

(34) Andrews, L.; Tague, T. J., Jr. *J. Am. Chem. Soc.* **1994**, *116*, 6856.

Table 3. Calculated Relative Energies and Geometries for $ScCO_2$ and $ScCO_2^+$ Isomers and $OScCO^-$

method	molecule	relative energy (kcal/mol)	geometry
BP86	OScCO ($^2A''$)	0	O−Sc, 1.690 Å; Sc−C, 2.205 Å; C−O, 1.172 Å; ∠OScC, 110.0°; ∠ScCO, 179.8°
	O′Sc[CO] ($^2A'$)	+6.4	O′−Sc, 1.685 Å; Sc−C, 2.349 Å; Sc−O, 2.238 Å; C−O, 1.211 Å; ∠O′ScC, 116.4°; ∠O′ScO, 115.3°
	Sc[OC]O′ ($^2A'$)	+13.6	Sc−O, 1.873 Å; Sc−C, 2.111 Å; C−O, 1.431 Å; C−O′, 1.199 Å; ∠OScC, 41.6°; ∠OCO′, 125.7°
	Sc[OO]C ($^2A_1$)	+15.3	Sc−O, 1.921 Å; C−O, 1.364 Å; ∠OScO, 36.0°; ∠OCO, 111.8°
	OScCO ($^4A''$)	+67.0	O−Sc, 1959 Å; Sc−C, 2.140 Å; C−O, 1.176 Å; ∠OScC, 122.3°; ∠ScCO, 170.9°
	O′Sc[CO] ($^4A'$)	+78.5	O′−Sc, 1.947 Å; Sc−C, 2.223 Å; Sc−O, 2.213 Å; C−O, 1.208 Å; ∠O′ScC, 117.4°; ∠O′ScO, 131Å
	$OScCO^+$ ($^1A'$)	+144.4	O−Sc, 1.639 Å; Sc−C, 2.451 Å; C−O, 1.129 Å; ∠OScC, 89.8°; ∠ScCO, 170.7°
	$OScOC^+$ ($^1A'$)	+151.7	O−Sc, 1.631 Å; Sc−O, 2.360 Å; O−C, 1.155 Å; ∠OScO, 104.8°; ∠ScOC, 172.1°
	$ScOCO^+$ ($^1\Sigma^+$)	+163.4	Sc−O, 1.623 Å; O−C, 5.117 Å; C−O, 1.139 Å
	$ScOOC^+$ ($^1\Sigma^+$)	+163.7	Sc−O, 1.623 Å; O−O, 4.533 Å; O−C, 1.141 Å
	$OScCO^-$ ($^3A''$)	−28.8	O−Sc, 1.721 Å; Sc−C, 2.257 Å; C−O, 1.185 Å; ∠OScC, 109.9°; ∠ScCO, 182.7°
B3LYP	OScCO ($^2A''$)	0	O−Sc, 1.680 Å; Sc−C, 2.217 Å; C−O, 1.159 Å; ∠OScC, 113.9°; ∠ScCO, 179.8°
	OSc[CO] ($^2A'$)	+5.0	O′-Sc, 1.676 Å; Sc−C, 2.362 Å; Sc−O, 2.219 Å; C−O, 1.201 Å; ∠O′ScC, 119.7°; ∠O′ScO, 118.4°
	Sc[OC]O ($^2A'$)	+12.3	Sc−O, 1.887 Å; Sc−C, 2.113 Å; C−O, 1.386 Å; C−O′, 1.191 Å; ∠OScC, 40.1°; ∠OCO′, 127.4°
	$OScCO^+$ ($^1A'$)	+140.8	O−Sc, 1.625 Å; Sc−C, 2.497 Å; C−O, 1.117 Å; ∠OScC, 94.4°; ∠ScCO, 172.1°
	$OScOC^+$ ($^1A'$)	+145.8	O−Sc, 1.621 Å; Sc−O, 2.354 Å; O−C, 1.143 Å; ∠OScO, 106.5°; ∠ScOC, 171.3°

Table 4. Calculated Vibrational Frequencies (cm^{-1}) and Intensities (km/mol) for the Structures Described in Table 3

	molecule	frequencies (intensities)
BP86	OScCO ($^2A''$)	99.2 (24), 230.8 (1), 280.8 (1), 383.9 (18), 917.4 (252), 1912.7 (559)
	OSc[CO] ($^2A'$)	129.3 (25), 160.2 (13), 320.8 (19), 346.6 (12), 929.3 (249), 1648.6 (266)
	Sc[OC]O ($^2A'$)	303.3 (6), 337.4 (0), 368.3 (70), 618.2 (22), 829.5 (130), 1761.8 (584)
	Sc[OO]C ($^2A_1$)	304.7 (0.3), 359.8 (4), 476.6 (48), 753.2 (11), 927.5 (248), 995.4 (4)
	OScCO ($^4A''$)	108.6 (7), 288.2 (5), 299.9 (11), 366.0 (51), 579.1 (125), 1818.2 (2421)
	$OScCO^+$ ($^1A'$)	79.5 (34), 217.3 (1), 246.3 (21), 289.4 (17), 1009.9 (118), 2210.6 (56)
	$OScOC^+$ ($^1A'$)	73.6 (27), 145.0 (6), 165.2 (5), 224.2 (51), 1025.1 (139), 2011.7 (249)
	$ScOCO^+$ ($^1\Sigma^+$)	12.7 (5), 24.1 (2 × 6), 40.6 (2 × 46), 1041.2 (136), 2130.2 (72)
	$ScOOC^+$ ($^1\Sigma^+$)	13.7 (5), 25.6 (2 × 2), 41.2 (2 × 49), 1040.8 (137), 2112.2 (89)
	$OScCO^-$ ($^3A''$)	92.3 (2), 234.2 (2), 271.0 (5), 345.3 (15), 862.1 (185), 1821.5 (709)
B3LYP	OScCO ($^2A''$)	100.7 (28), 224.7 (1), 282.2 (2), 387.1 (20), 945.0 (374), 1975.8 (798)
	OSc[CO] ($^2A'$)	131.4 (33), 161.4 (16), 339.1 (26), 353.2 (12), 959.1 (333), 1688.5 (391)
	Sc[OC]O ($^2A'$)	318.9 (5), 360.7 (0), 433.5 (48), 690.1 (57), 875.6 (185), 1805.4 (777)
	$OScCO^+$ ($^1A'$)	77.5 (36), 219.8 (1), 236.9 (29), 275.6 (15), 1052.6 (159), 2312.6 (48)
	$OScOC^+$ ($^1A'$)	77.7 (30), 149.3 (8), 169.4 (8), 233.7 (54), 1060.8 (179), 2097.3 (277)

than the inserted cation $OScCO^+$. These are described in Tables 3 and 4 as $OScOC^+$ ($^1A'$) and $ScOCO^+$ ($^1\Sigma^+$) and are calculated to be 151.7 and 163.4 kcal/mol, respectively, above OScCO ($^2A''$). The more stable $OScOC^+$ species is predicted to have lower modes, 2011.7 and 1025.1 cm^{-1}, whereas the less stable $ScOCO^+$ isomer is calculated to have higher frequencies, 2130.2 and 1041.2 cm^{-1}. These calculations correlate with the above observed band pairs, 2068.1 and 974.1 cm^{-1} for $OScOC^+$ and 2105.7 and 976.4 cm^{-1} for $ScOCO^+$. The calculated 12/13 and 16/18 ratios are in excellent agreement with the observed values. The observed/calculated (BP86) scale factors for the Sc−O stretching modes of the three cations in order of increasing energy are 0.956, 0.950, and 0.938, and the scale factors for the C−O stretching modes likewise are 1.005, 1.028, and 0.988 for these cation species.

$OYOC^+$ and $YOCO^+$. Two analogous weak bands at 2106.0 and 2078.0 cm^{-1} and their associated 871.9 and 869.1 cm^{-1} absorptions exhibit the same behavior as the scandium species. These bands are assigned, respectively, to $YOCO^+$ and $OYOC^+$ cations.

Table 5. Comparison of Observed and Calculated (BP86/6-311+G*) Isotopic Frequency Ratios for Sc−O and C−O Stretching Fundamentals of OScCO and OSc[CO] Molecules and $OScCO^+$ Cations and Calculated Ratios for $OScCO^-$

molecule	vibrational mode	12−16/13−16 obsd	12−16/13−16 calcd	12−16/12−18 obsd	12−16/12−18 calcd
OScCO	Sc−O stretch	1.00000	1.00000	1.04346	1.04380
	C−O stretch	1.02338	1.02349	1.02277	1.02366
OSc[CO]	Sc−O stretch	1.00000	1.00000	1.04324	1.04369
	C−O stretch	1.02230	1.02283	1.02450	1.02468
Sc[OC]O	Sc−O stretch	1.00934	1.00924	1.03886	1.03778
	C−O stretch	1.02440	1.02383	1.01948	1.02299
$OScCO^+$	Sc−O stretch	1.00000	1.00000	1.04356	1.04382
	C−O stretch	1.02288	1.02314	1.02392	1.02428
OSc^+OC	Sc−O stretch	1.00000	1.00000	1.04349	1.04378
	C−O stretch	1.02234	1.02278	1.02442	1.02470
ScO^+CO	Sc−O stretch	1.00000	1.00000	1.04373	1.04381
	C−O stretch	1.02248	1.02281	1.02447	1.02473
$OScCO^-$	Sc−O stretch	not	1.00000	not	1.02277
	C−O stretch	not	1.04379	not	1.02472

Other Absorptions. The 1652.7 and 1657.0 cm^{-1} bands observed in both Sc and Y (and other transition metal) experiments on deposition decreased on 25 K annealing, decreased on photolysis using 470-nm long-wavelength pass filter, and disappeared with the full arc. These bands show large carbon isotopic ratios (1.02729 and 1.02734) and small oxygen isotopic ratios (1.01705 and 1.01700). In the mixed $^{12}C^{16}O_2 + {}^{13}C^{16}O_2$ experiment, doublets were observed, while 1/2/1 triplets were observed in the mixed $^{12}C^{16}O_2 + {}^{12}C^{16,18}O_2 + {}^{12}C^{18}O_2$ experiment. These isotopic data indicate the CO_2 stoichiometry and assignment of the 1657.0 cm^{-1} band to the antisymmetric stretching vibration of the isolated CO_2^- molecular anion, which has been observed at 1658.3 cm^{-1} in a neon matrix.[22] The 1652.7 cm^{-1} band is due to a $(CO_2^-)(CO_2)_x$ cluster.[23] Electrons produced in the laser ablation process are available for capture by small molecules during condensation to form molecular anions.[35,36]

Two weak bands at 1856.7 and 1184.7 cm^{-1} appeared on annealing at the expense of CO_2^- absorptions, decreased on photolysis with 470-nm long-wavelength pass filter, and vanished on full arc photolysis. These two bands tracked together and were observed in other metal experiments.[23] The isotopic ratios for the upper band (12/13, 1.02785; 16/18, 1.01637) indicate an antisymmetric CO_2 vibration, while the lower band

Scheme 1

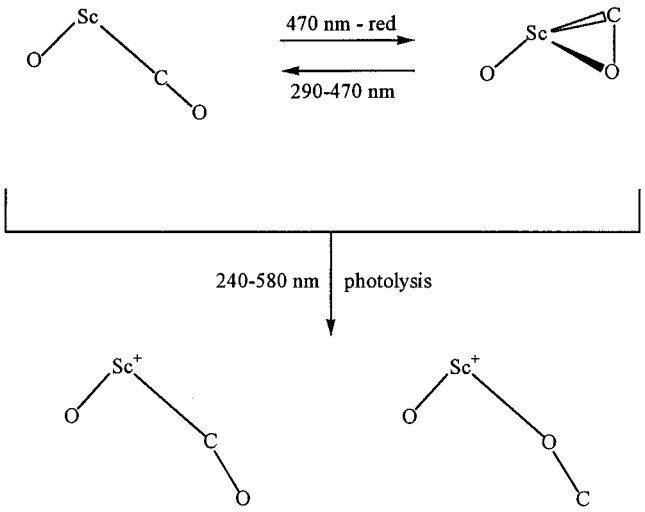

ratios (12/13, 1.00629; 16/18, 1.04794) implied a symmetric CO_2 vibration. Doublet and triplet isotopic absorptions were observed for the upper band using mixed $^{12}C^{16}O_2 + {}^{13}C^{16}O_2$ and $^{12}C^{16}O_2 + {}^{12}C^{16,18}O_2 + {}^{12}C^{18}O_2$ samples, while triplet and sextet isotopic multiplets were observed for the lower mode. These two bands are due to the symmetric $C_2O_4^-$ molecular anion with D_{2d} structure.[23]

Reaction Mechanisms. As predicted by theoretical calculations, Sc insertion into CO_2 to form the OScCO molecule (reaction 1a) is the dominant process, which was calculated to be exothermic by about 29 kcal/mol.[14] A trace of the addition product Sc-(η^2-OC)O is observed as well, and this reaction 1b is exothermic by only 15 kcal/mol.

$$Sc + CO_2 \rightarrow OScCO \quad (1a)$$

$$Sc + CO_2 \rightarrow Sc\text{-}(\eta^2\text{-}OC)O \quad (1b)$$

In both Sc and Y experiments, the insertion and addition product molecule absorptions increased on annealing, indicating that reactions 1 can proceed without activation energy in accord with calculations.[15] Although the Sc atom interaction with CO_2 to form the Sc-(η^2-OO)C complex is energetically favorable,[14] none of the latter product was observed here presumably due to the greater stability of the insertion product on the overall potential energy surface. This surface has been explored in detail by density functional calculations for the Ti + CO_2 reaction,[37] where the Ti-(η^2-OC)O intermediate adduct spontaneously inserts to form OTiCO, and experiments show that OTiCO is the major product of this reaction.[17] Finally, there is no evidence for $O_2Sc(CO)_2$ species involving two CO_2 subunits analogous to $O_2Cr(CO)_2$ reported earlier,[18] presumably owing to the lower stability of ScO_2.

The OM-(η^2-CO) molecules were formed by photolysis using the 470-nm long-wavelength pass filter, while the OMCO absorptions were almost destroyed. This suggests photoisomization reaction 2a, which was calculated to be slightly endothermic for Sc (6.4 kcal/mol by BP86 and 5.0 kcal/mol by B3LYP). This photoexcitation probably involves an n $\rightarrow \pi^*$ type transition on the CO subunit as the metal forms an additional bond to oxygen.

$$OMCO + h\nu \rightarrow [OMCO]^* \xrightarrow{\text{rearrange}} [OM\text{-}(\eta^2\text{-}CO)]^* \xrightarrow{\text{relax}} OM\text{-}(\eta^2\text{-}CO) \quad (2a)$$

The OM-(η^2-CO) absorptions were destroyed on full arc photolysis, while some of the OMCO absorbance was restored; this means that reaction 2a can also be reversed using higher energy photons (reaction 2b).

$$OM\text{-}(\eta^2\text{-}CO) + h\nu \rightarrow [OM\text{-}(\eta^2\text{-}CO)]^* \xrightarrow{\text{rearrange}} [OMCO]^* \xrightarrow{\text{relax}} OMCO \quad (2b)$$

The $OMCO^+$ and $OMOC^+$ cations were produced on full arc photolysis at the expense of OM-(η^2-CO) (Figure 1c,d). This suggests that the $OMCO^+$ and $OMOC^+$ cations were formed by photoionization of bridged OM-(η^2-CO) molecules (reaction 2c), which can give both cation structures. Scheme 1 summarizes the photochemistry.

$$[O\text{-}M\text{-}(\eta^2\text{-}CO)]^* + h\nu \rightarrow OMCO^+ \text{ and } OMOC^+ + e^- \quad (2c)$$

Since the calculated ionization energy of OScCO (144 kcal/mol) exceeds the mercury arc energy (119 kcal/mol at 240 nm), it is probable that an [OM-(η^2-CO)]* excited state, which can relax to the OM-(η^2-CO) isomer (reaction 2a), is sufficiently long-lived to absorb a second photon to reach ionization (reaction 2c). This also appears to be the case for the Ti and V/CO_2 systems where the cations are formed on full arc photolysis involving the [OM-(η^2-CO)]* intermediate structure.[38] In this regard, the ^{4}A states of OScCO and OSc-(η^2-CO) are 67.0 and 78.5 kcal/mol above the ^{2}A ground states and should have long enough lifetimes to absorb a second photon. Absorption into higher doublet states could access these quartet states through intersystem crossing.

The $OMCO^+$, $OMOC^+$, and $MOCO^+$ molecular cation absorptions were very weak on deposition, which suggests that reactions of Sc^+ cations from laser ablation[39] with CO_2 molecules to form $OMCO^+$, $OMOC^+$, and $MOCO^+$ (reactions 3) play a minor role. Reaction 3a was calculated for Sc^+ to be exothermic by about 50kcal/mol,[16] and the small increase in $OMCO^+$ on 25 K annealing may also be due to this reaction. On the other hand, direct photoionization of OScCO by hard ultraviolet radiation in the laser plume can account for the small initial yield of $OScCO^+$, but not $OScOC^+$, as the OScOC neutral molecule was not observed here.

$$M^+ + CO_2 \rightarrow OMCO^+ \quad (3a)$$

$$M^+ + CO_2 \rightarrow OMOC^+ \quad (3b)$$

$$M^+ + CO_2 \rightarrow MOCO^+ \quad (3c)$$

Experiments performed with CCl_4 added to the reagent mixture (0.5% CO_2, 0.1% CCl_4) increased the yields of $OScCO^+$, $OScOC^+$, and $ScOCO^+$ cation absorptions produced on full-arc photolysis 2-fold relative to OScCO bands. Carbon tetrachloride is an excellent electron scavenger, and electrons produced in photochemical reaction 2c are captured by CCl_4

(35) Chertihin, G. V.; Andrews, L. *J. Chem. Phys.* **1998**, *108*, 6404.
(36) Andrews, L.; Zhou, M. F.; Willson, S. P.; Kushto, G. P.; Snis, A.; Panas, I. *J. Chem. Phys.* **1998**, *109*, 177.
(37) Papai, I.; Mascetti, J.; Fournier, R. *J. Phys. Chem. A* **1997**, *101*, 4465.
(38) Zhou, M. F.; Andrews, L., submitted (Ti, V + CO_2).
(39) Thiem, T. L.; Salter, R. H.; Gardner, J. A. *Chem. Phys. Lett.* **1994**, *218*, 309.
(40) Zhou, M. F.; Andrews, L. *J. Chem. Phys.* **1998**, in press.

(as CCl_3 and Cl^-) and cannot neutralize cation products. Furthermore, electrons produced by laser ablation are also captured by CCl_4, and therefore, more Sc^+ produced on ablation can survive to undergo reactions 3. In similar studies with Fe, Ni, and CO, anions are eliminated from the product spectrum on CCl_4 doping and cation absorptions are increased relative to the neutral counterpart.[40,41]

Conclusions

Laser-ablated Sc and Y atoms react with CO_2 molecules to give primarily the insertion product OScCO and OYCO molecules, which have been isolated in a solid argon matrix. Photoisomerization to form OM-(η^2-CO) and ionization with a second photon to $OMCO^+$, $OMOC^+$, and $MOCO^+$ cations proceeded upon different wavelength photolyses. The product absorptions were identified by isotopic substitution and BP86 and B3LYP density functional calculations of isotopic frequencies to provide an experimental and theoretical match of normal vibrational modes of new molecules. Agreement between BP86 and B3LYP calculations is a good indication that these systems are well defined.

Acknowledgment. We gratefully acknowledge NSF support under Grant CHE 97-00116.

JA982900+

(41) Zhou, M. F.; Andrews, L. *J. Am. Chem. Soc.* **1998**, in press.